Sensitivity of the Himalayan orography representation in simulation of winter precipitation using Regional Climate Model (RegCM) nested in a GCM

P.R. Tiwari[1], S.C. Kar[2*], U.C. Mohanty[3], S. Dey[1], P. Sinha[4] and M.S. Shekhar[5]

[1]Centre for Atmospheric Sciences, IIT Delhi, India

[2]National Centre for Medium Range Weather Forecasting, Noida, India

[3]School of Earth Ocean and Climate Sciences, IIT Bhubaneswar, India

[4]Indiana State Climate Office, Purdue University, USA

[5]Snow and Avalanche Study Establishment, Chandigarh, India

*Correspondence
Dr. S.C. Kar
National Centre for Medium Range Weather Forecasting (NCMRWF),
A-50, Sector-62, Noida, India
Email: sckar@ncmrwf.gov.in

Abstract

The role of the Himalayan orography representation in a Regional Climate Model (RegCM4) nested in NCMRWF global spectral model is examined in simulating the winter circulation and associated precipitation over the Northwest India (NWI; 23^0 – 37.5^0N and 69^0 – 85^0E) region. For this purpose, nine different set of orography representations for nine distinct precipitation years (three years each for wet, normal and dry) have been considered by increasing (decreasing) 5%, 10%, 15% and 20% from the mean height (CNTRL) of the Himalaya in RegCM4 model. Validation with various observations revealed a good improvement in reproducing the precipitation intensity and distribution with increased model height compared to the results obtained from CNTRL and reduced orography experiments. Further it has been found that, increase in height by 10% (P10) increases seasonal precipitation about 20%, while decrease in height by 10% (M10) results around 28% reduction in seasonal precipitation as compared to CNTRL experiment over NWI region. This improvement in precipitation simulation comes due to better representation of vertical pressure velocity and moisture transport as these factors play an important role in wintertime precipitation processes over NWI region. Furthermore, a comparison of model-simulated precipitation with observed precipitation at 17 station locations has been also carried out. Overall, the results suggest that when the orographic increment of 10% (P10) is applied on RegCM4 model, it has better skill in simulating the precipitation over the NWI region and this model is a useful tool for further regional downscaling studies.

Key words: Northwest India, orography, precipitation and RegCM4.

1. Introduction

The short-term climate over mountain region is modulated mainly by complex topographical features and land surface characteristics (Pielke and Avissar 1990; Giorgi and Mearns 1991; Giorgi and Avissar 1997; Im and Ahn 2011) as well as non-linear interactions between small scales to planetary scale physical processes (Namias 1960; Smith 1979; Kasahara 1980; Wallace 1987). A number of theoretical studies are made to understand the upper air circulation features and associated precipitation over the mountain region (Fraser et al. 1973; Hobbs et al. 1973; Kasahara 1980). Sensitivity experiments on different land surface parameters (land use, vegetation covers, snow covers etc.) and orography using Global Circulation Models (GCMs) indicate that later plays most important role in representing space-time distribution of precipitation over the mountain region (Fennessy et al. 1994). Several modeling studies confirmed that orography representation governs spatial distribution of precipitation over many areas of the globe (Namias 1980, Roads and Maisel 1991). Kasahara and Washington (1968) have provided a detailed description about the thermal and dynamical effects of the orography in general circulation model. Later, a number of numerical experiments are conducted (Hahn and Manabe 1975; Chakraborty et al. 2002) to examine the role of the Himalayan mountain in the context of Indian summer monsoon circulation and associated precipitation. However, most of the studies are carried out with the assumptions of with and without orography using GCMs. A few modeling studies (Abe et al. 2003; Song et al. 2010) are conducted using GCMs as well as regional climate models (RCMs) to understand the changes in precipitation with the degree of changes in the mountain height. They found an increase in intensity of precipitation with the increase of model orography. However, these studies are focused on the summer monsoon season. It is also demonstrated in various studies that the modulation of rainfall over mountain region varies from low to high orographic features (Barros and Lettenmaier 1994).

A large part of northwest India is covered with the Western Himalayan (WH; 30^0 – 37.5^0N and 72^0 – 82^0E) region and the weather/climate over this region is complex due to high altitude and orientation of topography. During northern hemispheric winter seasons (December to February, DJF), large amount of precipitation occurs mostly in the form of snow over the Indian parts of WH region. The major contribution of seasonal precipitation comes from the eastward moving low-pressure synoptic systems known as Western Disturbances (WD; Pisharoty and Desai 1956; Chitlangia 1976). The WD originates over Mediterranean Sea and reaches to northwest India after passing through Iran, Afghanistan, and Pakistan during winter season. These synoptic weather systems are often fed by moisture from the Arabian Sea during its passage (Mohanty et al. 1998). When these moist reaches the WH region, forced ascent of moist air occurs which lead to the formation and growth of clouds and as a result large amount of precipitation takes place over this place. It is found that the seasonal precipitation amount is dependent on the large-scale fields that play a major role in the occurrence of WDs over this region (Revadekar and Kulkarni 2008). The amount of winter precipitation and its distribution has large impact in different sectors like agriculture, horticulture, transport, logistics etc as well as glacier basins that feed the rivers for storage of water. Therefore, monthly to seasonal scale predictions of precipitation intensity and distribution over NWI region is one of the important issues for policy planning and decision making to support the society and minimize the loss.

The regional climate models (RCMs) are used to simulate local/regional scale short-term climate worldwide. A brief description along with its advantages of present-day RCMs can be found in Rummukainen (2009) and performances of several RCMs in simulating Asian summer monsoon are well represented by Feng and Fu (2006) and Fu et al. (2005). It is well established that the skill of the RCMs are higher than Global Circulation Models (GCMs) due to better

representation of land surface characteristics and finer scale physical processes (Bhaskaran et al. 1996; Giorgi 2006; Tiwari et al. 2016). Since the atmospheric dynamics and physical forcing are resolved well in RCM than GCM, therefore short-term climate can be simulated well by RCM, especially, over the complex terrain (Giorgi and Bates 1989). Although, several experiments on sensitiveness of the orography in numerical weather predictions have been carried out (Hahn and Manabe 1975; Chakraborty et al. 2002; Abe et al. 2003), however most of these studies are focused on summer monsoon with the use of GCMs. A very few number of studies are reported so far to examine the performance of RCM in sub-grid scale in simulating winter circulation and associated precipitation over the NWI region (Sinha et al. 2015; Tiwari et al. 2014). The role of Himalayan height in a RCM to simulate winter circulation and associated precipitation is yet to be examined.

So, in the present study, regional climate model RegCM (version 4.1.1) developed at International Centre for Theoretical Physics (ICTP), Italy, is used to examine the changes in precipitation intensity and distribution by changing the Himalayan orography in the simulation of winter precipitation over the NWI region. For this purpose, nine distinct precipitation years (three years each for wet, normal and dry) have been considered. A brief description of the model and data used is provided in section 2. Methodology and discussion of results are given in section 3 and 4 respectively. And finally the concluding remarks including the findings in this study are given in section 5.

2. Model and data used

2.1 Model: Two models namely the NCMRWF global spectral model (T80) and International Centre for Theoretical Physics (ICTP) Regional Climate Model (RegCM) has been used in the

present study. The T80 model (atmosphere only model i.e. 2-tier) is the climate version of the medium-range weather forecast model of NCMRWF, India, which is one of the leading organizations to generate real-time forecast for the Indian region. This is a global spectral model with 80 waves in Triangular truncation (T80) and equivalent to 1.4° × 1.4° horizontal grid resolutions. To model the deep convection a fairly basic Kuo-Anthes type of cumulus scheme (Kuo 1974; Anthes 1977) is used. More details of the model can be found at Kanamitsu et al. (1991), Kar (2007) and Kar et al. (2011).

The regional climate model (RegCM4, version 4.1.1) used in the present study is developed at the Abdus Salam International Centre for Theoretical Physics (ICTP), consists of hydrostatic dynamical core similar to the fifth-generation Pennsylvania State University–National Center for Atmospheric Research Mesoscale Model (MM5) (Grell et al. 1994). It is a hydrostatic, terrain following model with state-of-the-art multiple physics options. The other model details can be found in Elguindi et al. (2011) and Giorgi et al. (2012). In this study we have used the cumulus scheme of Grell (1993) with Fritch–Chappell closure (Fritsch and Chappell 1980), land-surface scheme of Community Land Model or CLM3.5 (Oleson et al. 2008) and radiative transfer of the NCAR Community Climate Model version 3 (CCM3, Kiehl et al. 1996). The model domain and configuration used in this work are shown in Fig.1 and Table 1 respectively. The rectangular box drawn on Fig. 1 shows the area of interest for which results are analyzed. Figure 2 shows the differences in topography between T80 and RegCM models. The northwest to southeast oriented Himalayan ranges can be seen clearly distinguished in RegCM along with peaks and valleys more clearly than in the T80 model, where they appear to be absent.

In this study, the east–west extent of the RegCM model is up to 416 grid points and north–south extent is up to 320 grid points with center point of the model domain positioned at

15.1^0N/74.5^0E. The model integration is made from 1st November to 28th (29th for a leap year) of February of each year, for nine distinct winter seasons (three years each for wet, normal and dry) at 30 km model horizontal resolution. The initial and lateral boundary conditions from NCMRWF global spectral model (hereafter referred to as T80) have been used.

2.2 Data used: The model-simulated results are validated with the ERA-Interim reanalysis (hereafter referred to as ERA-Int; Dee et al. 2011) data, Indian Meteorological Department (IMD) gridded precipitation (0.25° × 0.25°) data (Pai et al. 2014) and station level data sets from Snow and Avalanche Study Establishment (SASE). It is to be stressed here that DJF seasonal rainfall data for a year is constructed by taking average of that year's December rainfall and next year's January and February rainfall. For example, values of 1982 DJF seasonal rain is obtained by averaging rainfall values of December 1982, January 1983 and February 1983**.** Furthermore, from the seasonal mean precipitation anomalies, extreme years (wet/dry) are selected on the basis of their departure from mean i.e. years having standardized precipitation anomaly greater than 1 are considered as wet, while years having less than -1 standardized precipitation anomaly are considered as dry years. Therefore, out of 28 years (1982-2009), there are 3 years in the category of wet (1991-92, 1994-95, 1997-98), 3 dry (1996-97, 2000-01, 2008-09) and 3 normal (1988-89, 1993-94, 2003-04) years. A composite analysis has been conducted by computing the precipitation anomaly pattern during wet/dry precipitation years. For comparison of model data with observation, model simulated results are interpolated bi-linearly to the grid points of the observed data.

3. Methodology

In order to investigate the sensitiveness of the Himalayan orography representation in simulating winter circulation and associated precipitation, nine sets of experiments with different

orography representations are carried out for each winter year. The representations of the orography are changed by increasing (reducing) by about +5% (-5%), +10% (-10%), +15% (-15%) and +20% (-20%) from the mean height of the Himalaya in RegCM model. The difference in Himalayan height after increasing by +10% from mean (control) height of the model is shown in Figure 3.

The mathematical expression for increasing (decreasing) of the Himalayan height is as follows:

$$H^* = H \pm \alpha \times H \quad \text{for} \quad H \geq 1.5km$$
$$= H \quad \text{for} \quad H < 1.5km \qquad \text{..... (1)}$$

Where H^* is the modified height of the Himalaya, the value of α is 0.1 and 0.2 for 10% and 20% increase or decrease from the mean height H. In the above expression, 'positive' ('negative') sign is for increase (decrease) of the orography. It may be noted that the mean height that is averaged over the whole Himalayan region is approximately 1.5 km (Abe et al. 2003), thus the height is changing when the H is equal to or greater than 1.5km.

The experiments with increased orography from the model mean height (CNTRL) by 5%, 10%, 15% and 20% are referred to as P5, P10, P15 and P20 experiments and experiments with reduced orography with the same amounts are referred to as M5, M10, M15 and M20 respectively. Several statistical analysis such as Hit Rate (HR), False Alarm Rate (FAR), Index of Agreement (IOA) and equitable threat score (ETS) have been computed in order to evaluate the performance of the model with various orography representation. It may be noted here that the model data is bi-linearly interpolated to the IMD grid points before carrying out the statistical computation. The mathematical expressions used for different statistical techniques are provided below:

Hit Rate (HR): This skill metrics gives that what fraction of the observed "yes" events were correctly forecasted. It is defined as,

$$HR = \frac{T}{T+F} \quad \text{..... (2)}$$

where T and F are hits, misses for each category. HR ranges from 0 to 1 with HR= 1 indicates perfect skill in prediction (i.e. F = 0).

False Alarm Rate (FAR): This skill metrics gives that what fraction of the observed "no" events were incorrectly forecasted as "yes". It is defined as,

$$FAR = \frac{NT}{NT+NF} \quad \text{..... (3)}$$

where NT and NF are number of false alarms and number of correct rejections. FAR ranges from 0 to 1 with FAR= 0 indicates perfect skill in prediction.

Index of agreement: Willmott (1982) stated that although the relative difference measures such as the ratio between RMSE and observed climatology frequently appear in the literature, they have the limitation that they are not bounded and are unstable for very small (near zero) climatology of observation. As a remedy, Willmott (1982) proposed new skill metrics called 'index of agreement (D)', as**:**

$$D=1-\left[\frac{\sum_i (M_i \quad O_i)^2}{\sum_i (|M_i \quad \overline{O}|+|O_i \quad \overline{O}|)^2}\right] \quad \text{..... (4)}$$

where M_i and O_i are the i^{th} year forecast and observation respectively and $\overline{O}$ is the observed climatology. This skill metric is relative and is bounded between 0 and 1 ($0 \leq D \leq 1$). The closeness of this index to 1 indicates the efficiency of the model in producing a good forecast.

Equitable Threat Score (ETS): ETS is one of the useful skill metrics to estimate the model performance, which is defined as (Wilks 1995):

$$ETS = \frac{(T \quad T)}{(T + M + F \quad T)} \text{ , where } T = \frac{(T + M) \quad (M + F)}{N} \qquad \text{..... (5)}$$

where M, T and F are number of misses, number of hits and number of false alarms for each category, hits due to random chance is denoted by T and N is the total number of events. ETS varies from −0.33 to 1. The value of ETS is equal to 0 (zero) indicates no skill and ETS is equal to 1 indicates perfect skill of the model in prediction.

4. Results and discussions

The results obtained from the RegCM model simulations with different orography representations are analyzed in this section. The detailed analysis of the model output is described into two broad sections namely i) circulation pattern and ii) precipitation.

4.1 Circulation pattern

The simulation of circulation features is carried with nine different orography representations (CNTRL, P5, P10, P15, P20, M5, M10, M15 and M20) in RegCM model. The difference between wet and dry year composites of seasonal mean (DJF) winds (at 500 hPa) for the nine sets of orography representation is shown in Figure 4. It is noticed that the observation has anomaly of stronger westerlies (> 2.5 m/s) over central part of India succeeded by cyclonic flow due to hindrance of the Himalayan orography (Fig. 4 a). It is worth mentioning here that the northern part of India receives precipitation when WDs passes over the region forming cyclonic anomaly over J&K and adjoining regions. The P10 model simulation (Fig. 4 d) is able to bring out the observed cyclonic flow feature better compared to the CNTRL experiment. Further an overestimation by about 2 m/s in P20 experiment and underestimation of wind with M5, M10, M15 and M20 experiments are noticed compare to observation.

The difference between wet and dry year composites of seasonal mean (DJF) meridional wind averaged over a longitudinal belt (from 28ºE to 128ºE) for the nine sets of orography representation is shown in ***Figure 5***. It is noticed from the diagram that at upper pressure levels (from 300-100 hPa) this component of wind is well brought out by P10 height (Fig. 4 d) as compared to the CNTRL and other orography representations. Further, where at one side there is an underestimation of about 2 m/s in CNTRL experiment compared to observations, there is an overestimation of the core of upper level wind by about 3 m/s in P20 experiment compared to observation. It is also noticed that the areas with stronger meridional winds are shifted southward (about 5^{o} shift in southward direction) in M5, M10, M15 and M20 experiments along with underestimation of the wind compared to ERA-Int. Overall, with the P10 orography representation the model simulations are closer to observations in terms of intensity, location and pattern of the zonal (Figure not shown) as well as meridional components of wind than the other orography representations in the model.

Figure 6 represents the longitude, height vertical cross-section of the differences between seasonal mean (DJF) wet- and dry-year composites of vertical pressure velocity (hereafter referred as omega) at 35^{o} N. Omega is one of the important upper air parameter that plays an important role in the model dynamics for precipitation simulation. Hence, it would be interesting to study the performance of the nine sets of orography representations in RegCM model in simulating the omega field. The orography of all nine set of representations in the RegCM simulations are also shown (in the black shaded bar). It can be noticed in ***Fig. 6*** that the vertical velocity maxima/minima is either over the valley bottom or along the upslope side of topography, which shows that the influence of the ridge–valley system on the vertical motion and hence precipitation formation processes. These vertical distributions across the Himalayan

region are more clearly brought out with enhanced orography in RegCM simulations compare to reduced orographic representations in RegCM model. This increased vertical motion could be one of the reasons for producing more (less) precipitation in enhanced orography in RegCM than the CNTRL or reduced orography in model during wet (dry) years. Furthermore, the sectorial (27ºN-38.5ºN) seasonal mean (DJF) differences between wet and dry year composites of zonal moisture transport at 500hPa from observation, and different Himalayan orography representations (CNTRL, P5, P10, P15, P20, M5, M10, M15 and M20) has been computed and shown in ***Fig. 7***. It can be noticed from the diagram that the Indian parts of Western Himalaya (IWH) region experiences a significant increase in zonal moisture transport with decreasing orography, which is brought in from westerly directions. Furthermore investigation indicates that model simulated precipitation is close to the observations with P10 height compared to other orographic representations in the RegCM4 model.

4.2 Precipitation

The changes in precipitation over the Northwest India (NWI) region with the changes in Himalayan orography are analyzed. For this purpose, model simulated area averaged (NWI) seasonal mean precipitation for total nine distinct winter seasons (three years each for wet, normal and dry) from nine sets of orographic representations have been computed and shown in ***Fig 8***. It is noticed from the figure that the area averaged seasonal precipitation increases with the increase of the Himalayan height over the NWI ($23^0 – 37.5^0$N and $69^0 – 85^0$E) region. Among nine orographic representations, RegCM model with P10 height simulates the precipitation amount closer to the observations over NWI region. Furthermore, model simulated seasonal mean precipitation and the Himalayan mean height both are averaged over the area bounded by 72°E-81°E and 29°N-37°N to see whether precipitation over the Indian parts of Western

Himalayan (IWH) region also changes with changes in Himalayan orography representations in the RegCM model. It is noticed from the ***Fig 9*** that the area averaged seasonal precipitation increases with the increase of the Himalayan height over the IWH region. Figure 8 also indicates that the increase in height by 10% (P10) causes an increase of precipitation by about 20%, while decrease in height by 10% (M10) causes a decrease of precipitation amount by 28% from CNTRL experiment. The reduction in height of the Himalaya allows stronger prevailing westerly wind on the leeward side that carries more moisture and hence less amount of precipitation occurs over the domain of interest.

The influence of the different orography representations in RegCM simulated spatial precipitation has been examined. For this purpose, the difference between wet and dry year composites of seasonal mean (DJF) precipitation have been computed and shown in ***Fig 10 (a-j)*** respectively. It is noticed that over the most parts of the domain of interest, a coherent positive precipitation pattern has emerged and this positive difference lies in the range of 1-4 mm/day with higher precipitation zone confined over Jammu and Kashmir (J&K) region (2-4 mm/day) in the observation (***Fig. 10a***). This observed precipitation is well brought in all the topographically enhancement experiments (for e.g. P5, P10, P15, P20) however the model is over estimating the precipitation as compared to the IMD observation. The higher precipitation over the J&K region is well depicted by the model. Over the Himachal Pradesh (HP) & Uttarakhand (UK) region, model simulation shows more precipitation (> 3 mm/day), while observation shows less precipitation (< 2mm/day). ***Figure 10 (g-j)*** reveals that the intensity of precipitation reduces (negative difference of about 1-4 mm/day over J&K, Punjab and HP regions) with the decrease in height of Himalaya over the region of interest. Over all, it is noticed that the precipitation intensity and distribution is represented better in P10 than other experiments of RegCM.

Furthermore, as previously mentioned, the northern part of India receives precipitation when WDs passes over the region forming cyclonic anomaly over J&K and adjoining regions. The P10 model simulation is able to bring out the observed cyclonic flow feature better compared to the other orographic representations.

It is of interest to study the spatial distribution and intensity of precipitation obtained from various experiments using statistical analysis. For this purpose various skill metrics for e.g. correlation coefficient (CC), RMSE, hit rate versus false alarm rate statistics, index of agreement (IOA) and equitable threat score (ETS) are computed for different orography experiments. A Taylor diagram (Taylor 2001) is presented in ***Figure 11***. In this diagram, the skill of the RegCM model in predicting the wintertime precipitation in terms of correlation, root mean square error (RMSE) and standard deviation is shown for the nine different sets of orographic representations (CNTRL, P5, P10, P15, P20, M5, M10, M15 and M20). The figure clearly depicts that the CC is maximum in P10 experiment with magnitude of 0.43, while minimum in M20 experiment with magnitude of 0.08.

An assessment of model simulated precipitation for various orography representtsions is made based on hit rate versus false alarm rate statistics and is shown in ***Figure 12***. For this purpose, a 2×2 contingency table is made in which forecast-observation pairs are classified into four different groups (Wilks 1995). It can be noticed from the diagram that the hit rate is maximum in P10 experiment with a hit rate (HR) of about 0.5 and minimum false alarm rate (FAR) of about 0.28. On the other hand the M20 experiment has least HR with a magnitude of 0.24 followed by M15, M10 and M5 experiments.

Further, in the present work, IOA skill metrics have been calculated for all nine different sets of orographic representations and is provided in ***Figure 13***. It is seen that among all

orographic representation experiments, P10 experiment has maximum IOA with a magnitude of 0.65. On the other hand, the IOA is minimum for M20 experiment and is a magnitude of 0.15. Furthermore, ETS has been also calculated for all the nine different sets of orographic representations and is provided in ***Figure 14***. The ETS has been computed for wet days and the wet day is considered when IMD precipitation is more than 1 mm/day. ***Figure 14*** shows that the ETS is maximum in P10 experiment (ETS=0.31) and minimum in M20 experiment (ETS=-0.11). It can be also noticed from the ***Fig. 14*** that the value of ETS is reducing with the reduced Himalayan orography in the RegCM model.

Over all, it is clear from the above statistical analysis that orography representation in the RegCM model plays an important role and a significant improvement in precipitation simulation comes with enhanced orographic representation. Further, maximum improvement in model-simulated precipitation comes over the domain of interest with P10 orographic representation.

4.3. Validation of model precipitation against station level observations

In this section, the RegCM4 model simulated precipitation with nine different sets of orography representations are validated against the Snow and Avalanche Study Establishment (SASE) observations over seventeen stations located over the Northwest Indian part of the Western Himalayas (IWH) region (***Fig. 15***). The gridded precipitation datasets obtained from the RegCM4 model with nine different sets of orography representations are bi-linearly interpolated to the station location for validation. Table 2 represents the station–wise seasonal mean precipitation obtained from SASE observation and RegCM4 simulated precipitation with CNTRL and P10 orographic representations. The shaded values of model simulation with CNTRL and P10 indicate the closest ones to the SASE observations. Further to a get deep insight, the Phase synchronizing events (PSE) has been computed for the RegCM4 performance

evaluation based on Table 2 results. The PSE method matches the sign (positive or negative) of the precipitation difference (composite of wet minus composite of dry years) obtained from SASE observations, CNTRL and P10 orographic representations to evaluate the performance of the RegCM4 model.

The computation of PSE is given below:

$$PSE = \left(\frac{P_e \quad P_e^{'}}{P_e} \right) \times 100 \qquad \text{……..(6)}$$

where P_e is the total number of events and P_e' is the number of events in the CNTRL and P10 orographic representations that have opposite in sign as compared to observations (out of phase). Thus, PSE=100 for the CNTRL and P10 results means that the sign of model anomalies (here the difference from composite of wet and dry years) is same as in the observations for all the stations and PSE=0 when none of the model results have a similar sign (i.e. either positive or negative both in model and observation) with observations. From the Table 2, it can be seen that the PSE value is maximum (with 88%) for composite (i.e., model output matches the sign of with observations 88% times) of wet minus dry years for P10 followed by CNTRL (with 71%) orographic representations. Overall, the RegCM4 simulated precipitation over seventeen stations is brought out well in P10 orographic representation experiment as compared to CNTRL experiment validated against SASE observation.

5. Conclusion

The influence of the Himalayan orography representation in regional climate model (RegCM4) on winter circulation and associated precipitation is studied over the NWI region. Nine different sets of orography representation such as Control (mean height of Himalaya in RegCM4; CNTRL), and 5%, 10%, 15% and 20% increase and decrease (P5, P10, P15 and P20, respectively for increase; M5, M10, M15 and M20 respective for decrease) of orography from

mean height (CNTRL) are considered to simulate nine distinct precipitation years (three years each for wet, normal and dry). The RegCM4 model is driven by NCMRWF global spectral model (T80) and the model-simulated results are validated with ERA-Int for circulation and IMD gridded as well SASE station level observations for precipitation. The major findings of the study are enumerated as follows:

- The RegCM4 model is able to represent seasonal mean circulation features in low as well as upper level reasonably well. However the strength of the circulation is weaker in CNTRL experiment when compared with the verification. Composites of wet minus dry year has been carried out which shows that the P10 model simulations are closer to observations in terms of intensity, location and pattern of the zonal as well as meridional components wind than other orographic representations in the RegCM4 model.
- To understand the possible reasons that are affecting the performance of the RegCM4 model simulations vertical pressure velocity and moisture transport are analyzed for composites of wet minus dry year and it is seen that these factors influence the precipitation during winter season over NWI region. While RegCM4 model with P10 height is able to demonstrate the above said features up to certain extent, the other combinations of orographic representations does not represent those features in a realistic manner.
- The RegCM4 simulated seasonal mean precipitation over the NWI region increases with the increase of orography. It is noted from the control experiment (CNTRL) of RegCM4 that increase in height by about 10% (P10) increases seasonal mean precipitation by about 20%, while decrease in 10% (M10) in height results around 28% reduction in seasonal mean precipitation as compared with CNTRL over NWI region. Further, seasonal mean

precipitation distribution during composites of wet minus dry year is computed over NWI region. It is noticed the precipitation intensity and distribution is brought out well in P10 experiment and is in good agreement with the IMD observation compared to other orographic representations in RegCM4 model.

- Statistical analysis such as hit rate versus false alarm rate statistics, index of agreement (IOA) and ETS suggests that the performance of RegCM4 model with 10% increase in Himalayan height (P10) is better in simulating precipitation over NWI region. Further, validation of model-simulated precipitation against SASE station level observations indicates that the RegCM4 model with P10 orographic representation is able to bring out precipitation amount closer to SASE observation over maximum number of stations (PSE value is maximum and is 88%).

Acknowledgements

We thank the anonymous reviewers for their comments and suggestions that helped us to

improve the manuscript. The RegCM4.1.1 model, installed at IIT Delhi, has developed at the ICTP, Trieste, Italy. Authors sincerely acknowledge the IMD and SASE for providing their daily gridded and station precipitation data. The authors would like to acknowledge European Centre for Medium-Range Weather Forecasts (ECMWF) for making their ERA-Interim data available to this study. The work is partly supported by research grant from Department of Science and Technology, Govt. of India under contract DST/CCP/PR/11/2011 through a research project operational at IIT Delhi (IITD/IRD/RP2580). The authors duly acknowledge Bianca C. for editing the English of the manuscript.

Reference

Abe M, Kitoh A, Yasunari T (2003) An Evolution of the Asian Summer Monsoon Associated with Mountain Uplift—Simulation with the MRI Atmosphere-Ocean Coupled GCM. J Meteorol Soc Japan 81: 909-933.

Anthes RA (1977) A cumulus parameterization scheme utilizing a one- dimensional cloud model. Mon Weather Rev 105: 270–286.

Barros AP, Lettenmaier DP (1994) Dynamic modeling of orographically induced precipitation. Rev Geophys 32: 265–284.

Bhaskaran B, Jones RG, Murphy JM, Noguer M (1996) Simulations of the Indian summer monsoon using a nested climate model: Domain size experiments. Clim Dyn 12: 573-587.

Chakraborty A, Nanjundiah RS, Srinivasan J (2002) Role of Asian and African orography in Indian summer monsoon. Geophys Res Lett 29: 10.1029/2002GL015522.

Chitlangia PR (1976) Mean Model of Western Depression. Indian Journal of Meteorology Hydrology and Geophysics 27 (2): 157-162.

Dee DP, Uppala SM, Simmons AJ, Berrisford P, Poli P, Kobayashi S, Andrae U, Balmaseda MA, Balsamo G, Bauer P, Bechtold P, Beljaars ACM, Van de Berg L, Bidlot J, Bormann

N, Delsol C, Dragani R, Fuentes M, Geer AJ, Haimberger L, Healy SB, Hersbach H, Hólm EV, Isaksen L, Kållberg P, Köhler M, Matricardi M, McNally AP, Monge-Sanz BM, Morcrette JJ, Park BK, Peubey C, Rosnay P, Tavolato C, Thépaut JN, Vitart F (2011) The ERA-Interim reanalysis: configuration and performance of the data assimilation system. Q J R Meteorol Soc 137: 553-597.

Elguindi N, Bi XQ, Giorgi F, Nagarajan B, Pal J, Solmon F, Rauscher S, Zakey A, Giuliani G (2011) Regional climatic model RegCM user manual version 4.1.1. The Abdus Salam International Centre for Theoretical Physics Strada Costiera, Trieste, Italy.

Fennessy MJ, Kinter JL, Kirtman B, Marx L, Nigam S, Schneider E, Shukla J, Straus D, Vernekar A, Xue Y, Zhou J (1994) The Simulated Indian Monsoon: A GCM Sensitivity Study. J Clim 7: 33–43.

Feng J, Fu C (2006) Inter-comparison of 10-year precipitation simulated by several RCMs for Asia. Adv Atmos Sci 23: 531-542.

Fraser AB, Easter RC, Hobbs PV (1973) A theoretical study of the flow of air and fallout of solid precipitation over mountainous terrain: Part I. Airflow model. J Atmos Sci 30: 801–812.

Fu C, Wang S, Xiong Z, Gutowski WJ, Lee DK, McGregor JL, Sato Y, Kato H, Kim JW, Suh MS (2005) Regional climate model intercomparison project for Asia. Bull Am Meteor Soc 86: 257-266.

Giorgi F, Bates GT (1989) The climatological skill of a regional climate model over complex terrain. Mon Weather Rev 117: 2325-2347.

Giorgi F, Mearns LO (1991) Approaches to the simulation of regional climate change: A review. Rev Geophys 29: 191–216.

Giorgi F, Avissar R (1997) The representation of heterogeneity effects in earth system modeling: Experience from land surface modeling. Rev Geophys 35: 413–438.

Giorgi F (2006) Regional climate modeling: status and perspectives. Journal de Physique IV (Proceedings) 139: 101–118.

Giorgi F, Coppola E, Solmon F, Mariotti L, Sylla MB, Bi X, Elguindi N, Diro GT, Nair V, Giuliani G, Cozzini S, Gu¨ttler I, O'Brien TA, Tawfik AB, Shalaby A, Zakey AS, Steiner AL, Stordal F, Sloan LC, Brankovic C (2012) RegCM4: model description and preliminary tests over multiple CORDEX domains. Clim Res 52: 7–29.

Grell GA (1993) Prognostic evaluation of assumptions used by cumulus parameterization. Mon Weather Rev 121: 764–787.

Grell GA, Dudhia J, Stauffer DR (1994) Description of the fifth generation Penn State/NCAR Mesoscale Model (MM5). Tech. Rep. TN-398+STR, NCAR, Boulder, Colorado, pp.1-12.

Hahn DG, Manabe S (19750 The Role of Mountains in the South Asian Monsoon Circulation. J Atmos Sci 32: 1515–1541.

Hobbs PV, Easter RC, Fraser AB (1973) A theoretical study of the flow of air and fallout of solid precipitation over mountainous terrain, II, Microphysics. J Atmos Sci 30: 813-823.

Holtslag AAM, De Bruijn EIF, Pan HL (1990) A high-resolution air mass transformation model for short-range weather forecasting. Mon Weather Rev 118: 1561–1575.

Im ES, Ahn JB (2011) On the elevation dependency of present day climate and future change over Korea from a high-resolution regional climate simulation. J Meteoro Soc 89: 89-100.

Kanamitsu M, Alpert JC, Campana KA, Caplan PM, Deaven DG, Iredell M, Katz B, Pan HL, Sela J, White WH (1991) Recent changes implemented into the global forecast system at NMC. Weather Forecast 6: 425–435.

Kasahara A, Washington WM (1968) Thermal and Dynamical Effects of Orography on the General Circulation of the Atmosphere, NCAR Manuscript, No. 68-208.

Kasahara A (1980) Influence of orography on the atmospheric general circulation, Orographic Effects in Planetary Flows. GARP Publ. Ser. 23, 3-49.

Kar SC (2007) Global model simulations of interannual variability of the Indian summer monsoon using observed SST variability. NCMRWF research Report, NMRF/RR/2/2007; 40 pp.

Kar SC, Iyengar GR, Bohra AK (2011) Ensemble spread and model systematic errors in the monsoon rainfall forecasts using the NCMRWF global ensemble prediction system. Atmosfer 24 (2): 173–191.

Kiehl JT, Hack JJ, Bonan GB, Boville BA, Briegleb BP, Williamson DL, Rasch PJ (1996) Description of the NCAR Community Climate Model (CCM3). NCAR Tech. Note NCAR/TN- 420+STR, 152 pp.

Kuo YH (1974) Further studies of the parameterization of the influence of cumulus convection of large-scale Flow. J Atmos Sci 31: 1232–1240.

Mohanty UC, Madan OP, Rao PLS, Raju PVS (1998) Meteorological fields associated with western disturbances in relation to glacier basins of western Himalayas during winter season. Technical Report, Centre for Atmospheric Science, IIT Delhi, India.

Namias J (1960) Synoptic and planetary scale phenomena leading to the formation and recurrence of precipitation, in Physics of Precipitation. Geophys. Monogr. Ser., 5, edited by H. Weickmann, pp. 32-44, AGU, Washington, D. C.

Namias J (1980) The art and science of long-range forecasting. Eos Trans. AGU 61: 449-450.

Oleson KW, Niu GY, Yang ZL, Lawrence DM, Thornton PE, Lawrence PJ, Stöckli R, Dickinson RE, Bonan GB, Levis S, Dai A, Qian T (2008) Improvements to the Community Land Model and their impact on the hydrological cycle. J Geophys Res 113: 1021-1026.

Pai DS, Sridhar L, Rajeevan M, Sreejith OP, Satbhai NS, Mukhopadhyay B (2014) Development of a new high spatial resolution ($0.25° \times 0.25°$) long period (1901-2010) daily gridded

rainfall data set over India and its comparison with existing data sets over the region. Mausam 65: 1–8.

Pielke R, Avissar R (1990) Influence of landscape structure on local and regional climate. Landscape Ecol 4: 133–155.

Pisaroty P, Desai BN (1956) Western Disturbance and Indian Weather. Indian Journal of Meteorology Hydrology and Geophysics 7: 333-338.

Revadekar JV, Kulkarni A (2008) The El Nino-Southern Oscillation and winter precipitation extremes over India. Int J Climatol 28: 1445–1452.

Roads JO, Maisel TN (1991) Evaluation of the National Meteorological Center's medium range forecast model precipitation forecasts. Weather Forecast 6: 123-130.

Rummukainen M (2009) State-of-the-art with regional climate models. WIREs Climate Change 1: 82-96.

Sinha P, Tiwari PR, Kar SC, Mohanty UC, Raju PVS, Dey S, Shekhar MS (2015) Sensitivity studies of convective schemes and model resolutions in simulations of wintertime circulation and precipitation over western Himalayas. Pure Appl Geophys 172 (2): 503-530.

Smith RB (1979) The influence of mountains on the atmosphere. Adv Geophys 21: 87-233.

Song JH, Kang HS, Byun YH, Hong SY (2010) Effects of the Tibetan Plateau on the Asian summer monsoon: a numerical case study using a regional climate model. Int J Climatol 30: 743-759.

Tiwari PR, Kar SC, Mohanty UC, Dey S, Sinha P, Raju PVS, Shekhar MS (2014) Dynamical downscaling approach for wintertime seasonal scale simulation over the western Himalayas. Acta Geophysica 62(4): 930-935.

Tiwari PR, Kar SC, Mohanty UC, Dey S, Sinha P, Raju PVS, Shekhar MS (2016) On the dynamical downscaling and bias correction of seasonal-scale winter precipitation predictions over North India. Q J R Meteo Soc DOI: 10.1002/qj.2832.

Wallace JM (1987) Observations of orographic influences upon large-scale atmospheric motions, in Seminar/Workshop 1986 on Observation, Theory and Modeling of Orographic Effects, vol. 1, pp. 23-49, European Centre for Medium-Range Weather Forecasts, Reading, England.

Wilks DS (1995) Statistical Methods in the Atmospheric Sciences. Academic Press: San Diego, CA; 467 pp.

Willmott CJ (1982) Some comments on the evaluation of model performance. Bull Am Meteorol Soc 63: 1309 –1313.

List of Figures

Figure 9: RegCM4 simulated area averaged (72°E-81°E; 29°N-37°N) seasonal (DJF) mean precipitation computed for different mean height of the Himalayan mountain representations (CNTRL, P5, P10, P15, P20, M5, M10, M15 and M20) respectively.

Figure 10:Seasonal mean (DJF) differences between wet- and dry-year composites of precipitation (mm/day) of (a) IMD observation, model simulations using (b) CNTRL, (c) P5, (d) P10, (e) P15, (f) P20, (g) M5, (h) M10, (i) M15 and (j) M20 heights respectively.

Figure 11: Taylor diagram for the north India average precipitation prediction skill of the different Himalayan orography representations.

Figure 12: Hit rate versus False alarm rate statistics computed for NWI region for nine different sets of Himalayan orography representations.

Figure 13: Willmott's index of agreement computed for NWI region for nine different sets of Himalayan orography representations.

Figure 14: Equitable threat score (ETS) computed for NWI region for nine different sets of Himalayan orography representations.

Figure 15: Geographical location of 17 SASE stations situated in the IWH region. (Source: The color geographical generated from http://woodshole.er.usgs.gov/mapit).

List of Tables

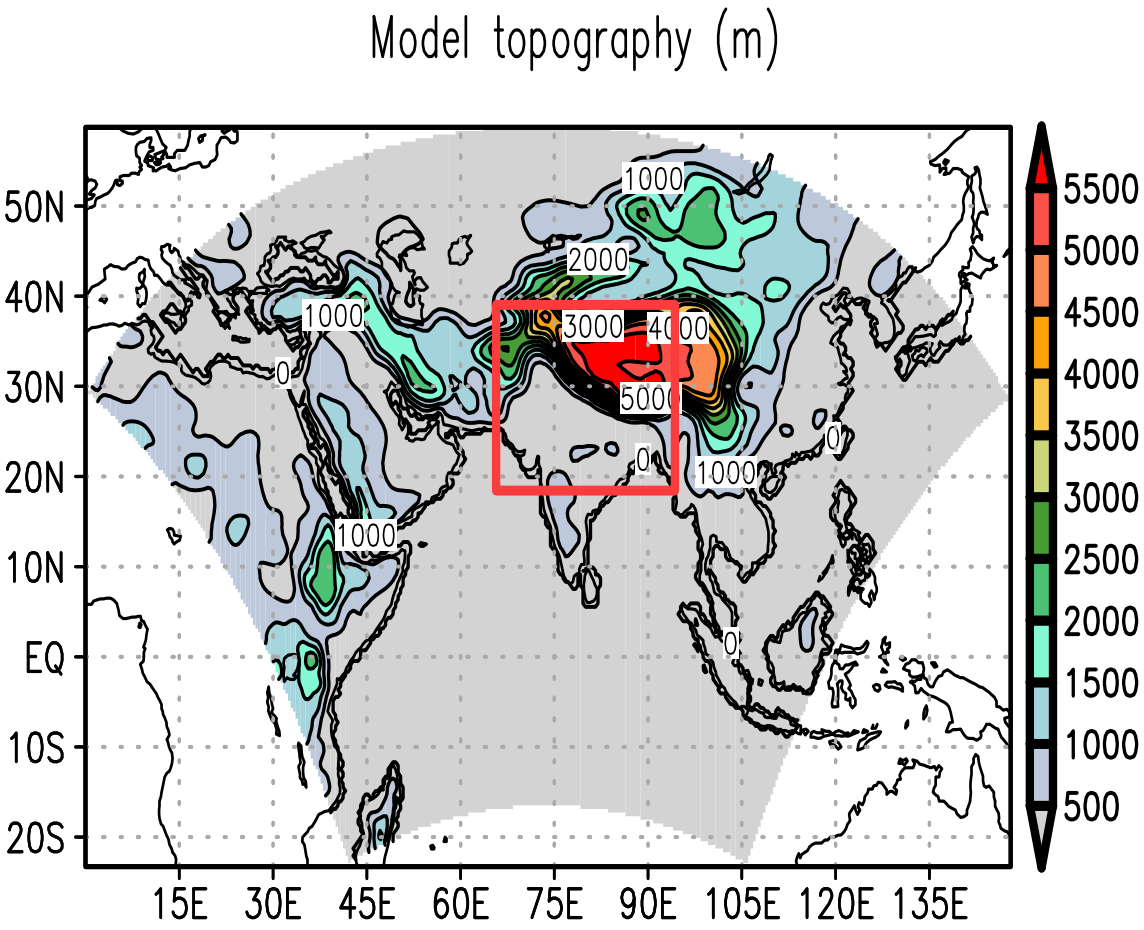

Figure 1: Topography (in m) and full model domain as used in RegCM. The region under the black box is the Northwest India region considered in the study. (Change the diagram same as of QJRMS with different color)

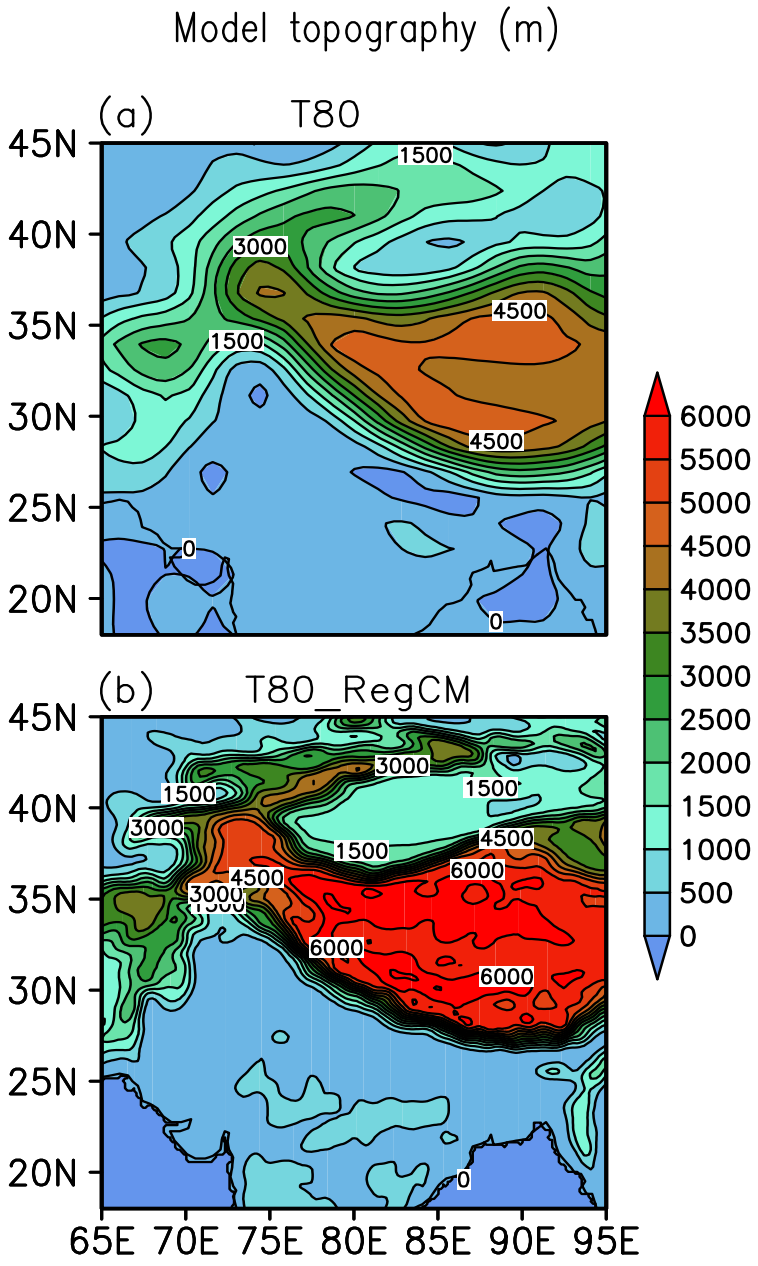

Figure 2: Model topography (in m) from (a) NCMRWF (T80) and (b) RegCM4 model respectively.

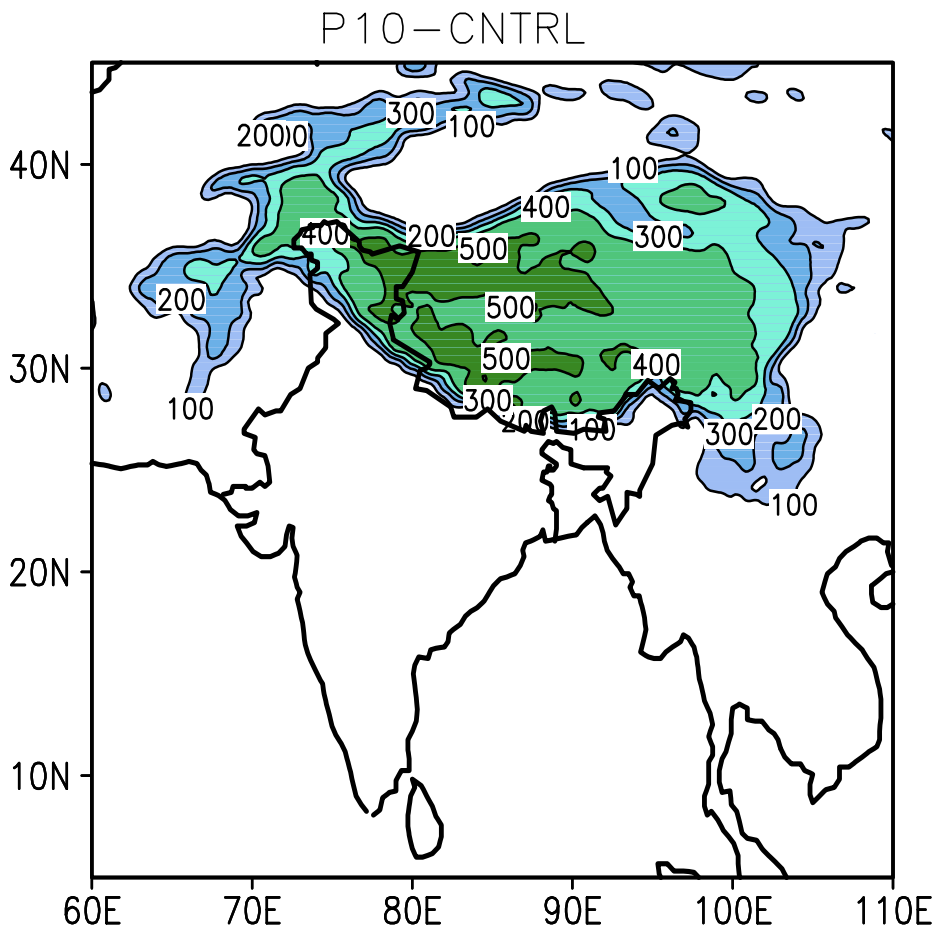

Figure 3: Height difference plot (in meters) over Himalayan region between RegCM model mean height and 10% increase from mean height of the model, with contour interval of 100m.

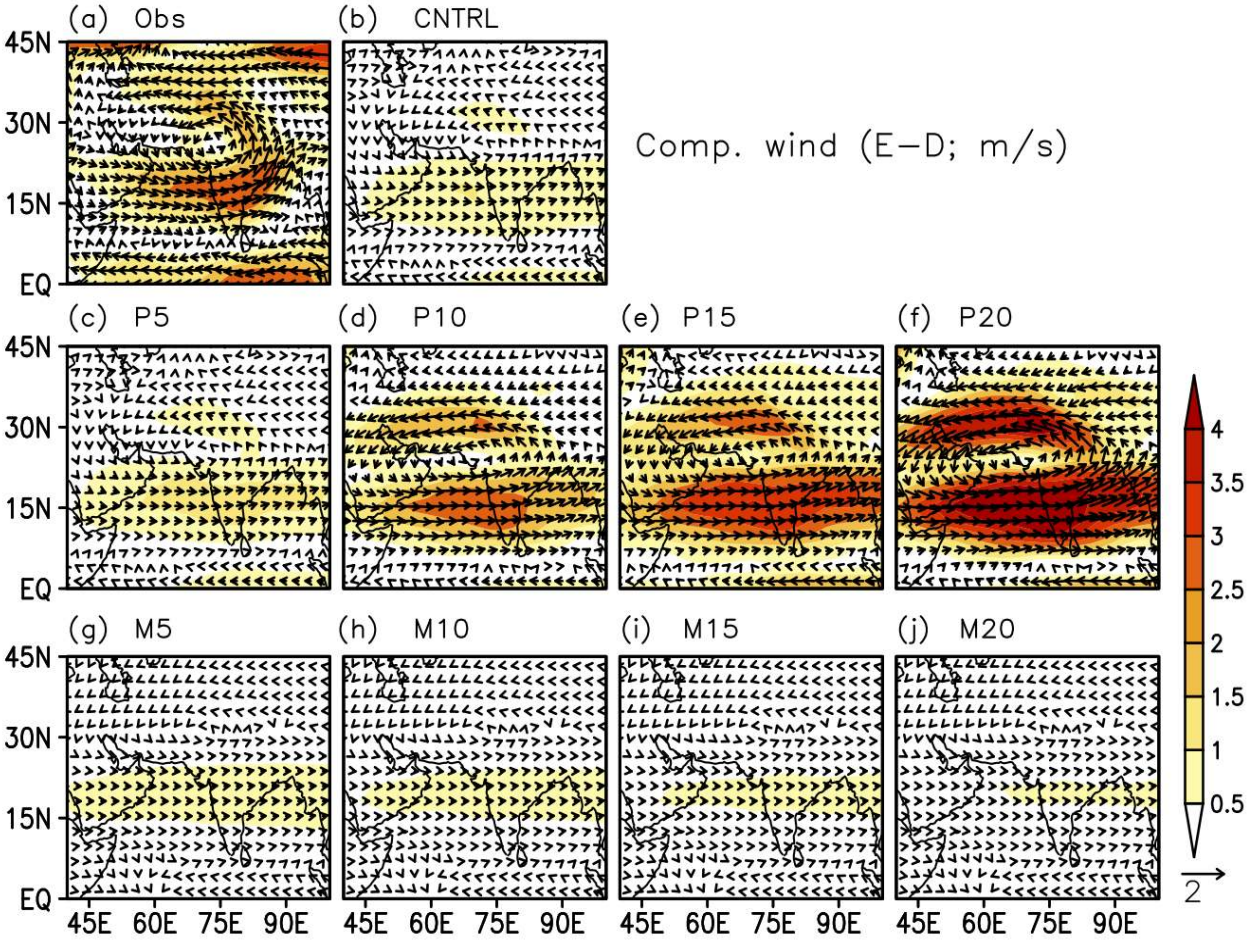

Figure 4: Seasonal mean (DJF) differences between wet- and dry-year composites of wind (in m/s) at 500 hPa from (a) ERA-Int, model simulations using (b) CNTRL, (c) P5, (d) P10, (e) P15, (f) P20, (g) M5, (h) M10, (i) M15 and (j) M20 heights respectively.

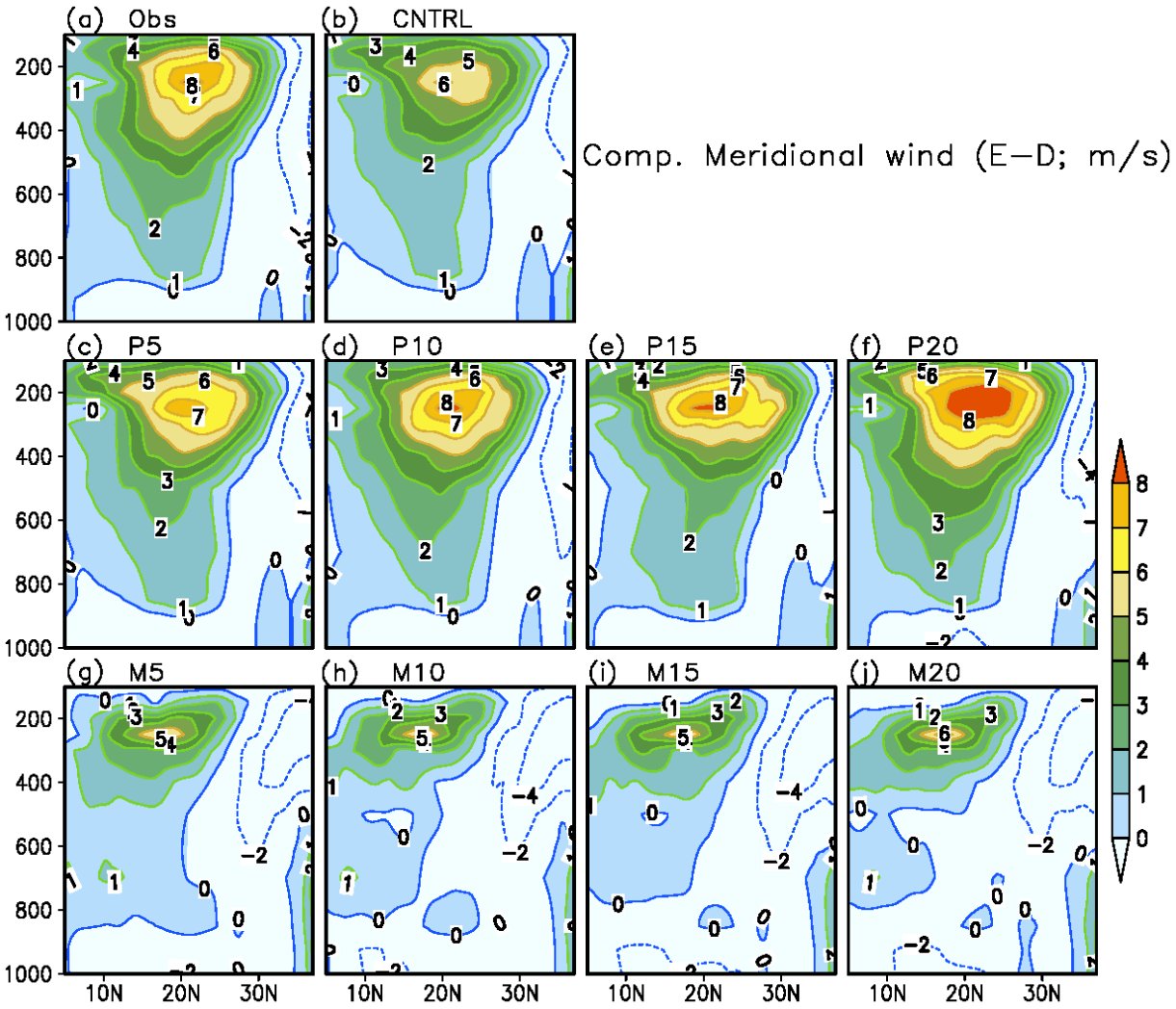

Figure 5: Sectorial (28ºE-128ºE) seasonal mean (DJF) differences between wet- and dry-year composites of meridional wind (in m/s) of (a) ERA-Int, model simulations using (b) CNTRL, (c) P5, (d) P10, (e) P15, (f) P20, (g) M5, (h) M10, (i) M15 and (j) M20 heights respectively.

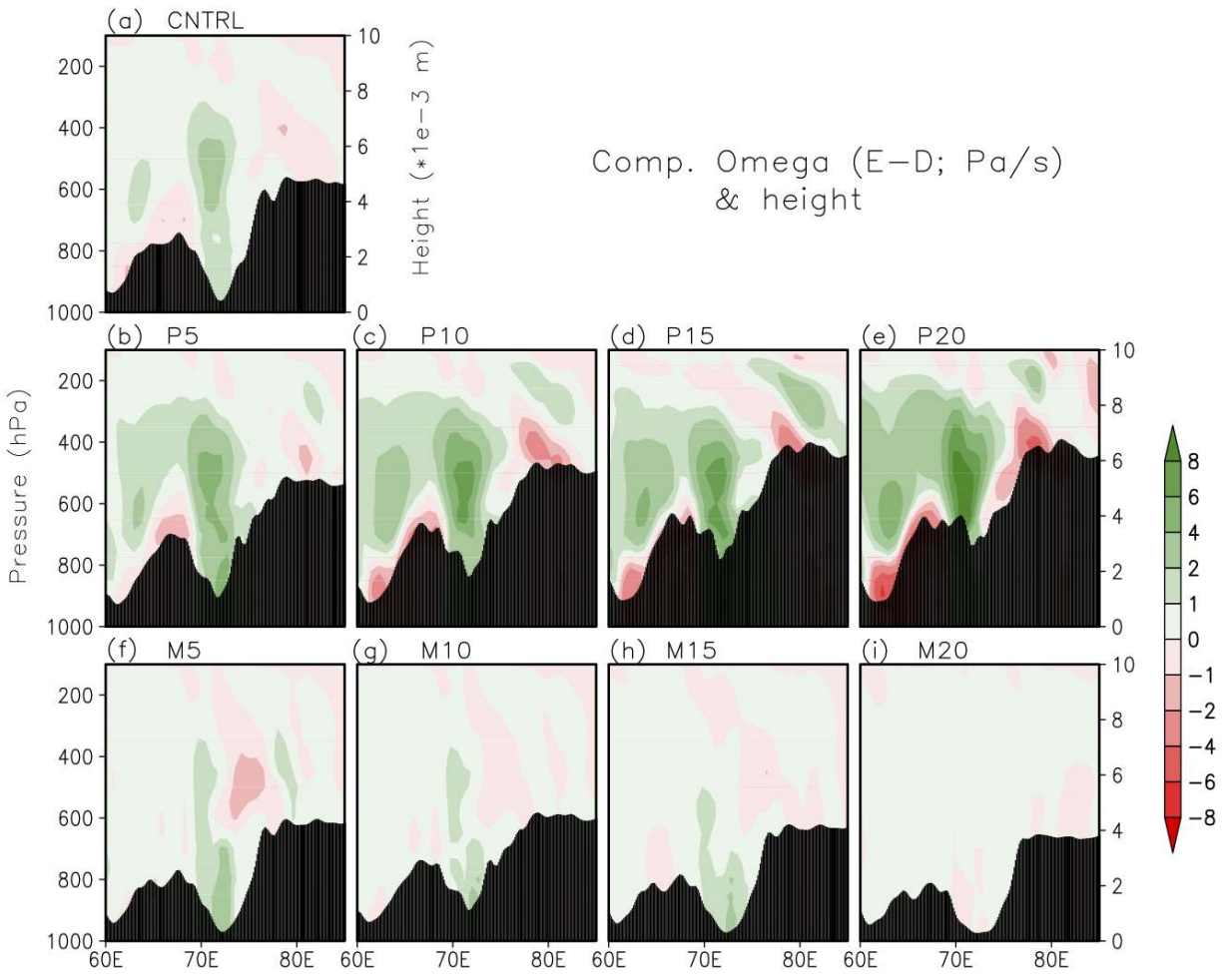

Figure 6: Longitude–height distribution of the differences between seasonal mean (DJF) wet- and dry-year composites of vertical velocity (Pa/s; shaded) and topography (*1e-3 m; shaded bar, right-hand vertical axis) in (a) CNTRL, (b) P5, (c) P10, (d) P15, (e) P20, (f) M5, (g) M10, (h) M15 and (i) M20 heights respectively at 35°N latitude.

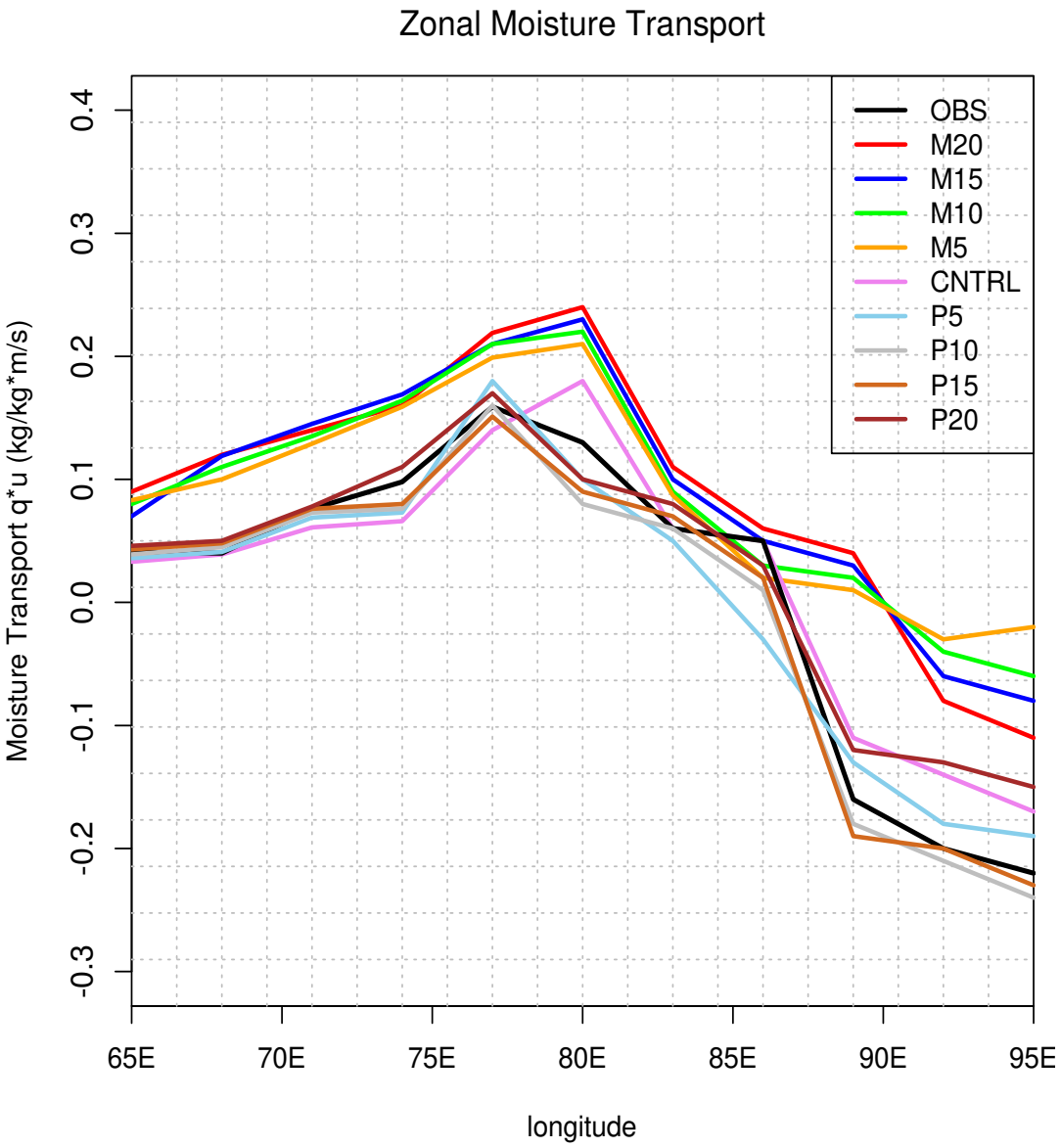

Figure 7: Sectorial (27ºN-38.5ºN) seasonal mean (DJF) differences between wet- and dry-year composites of zonal moisture transport at 500hPa obtained form observation and different Himalayan orography representations (CNTRL, P5, P10, P15, P20, M5, M10, M15 and M20) respectively.

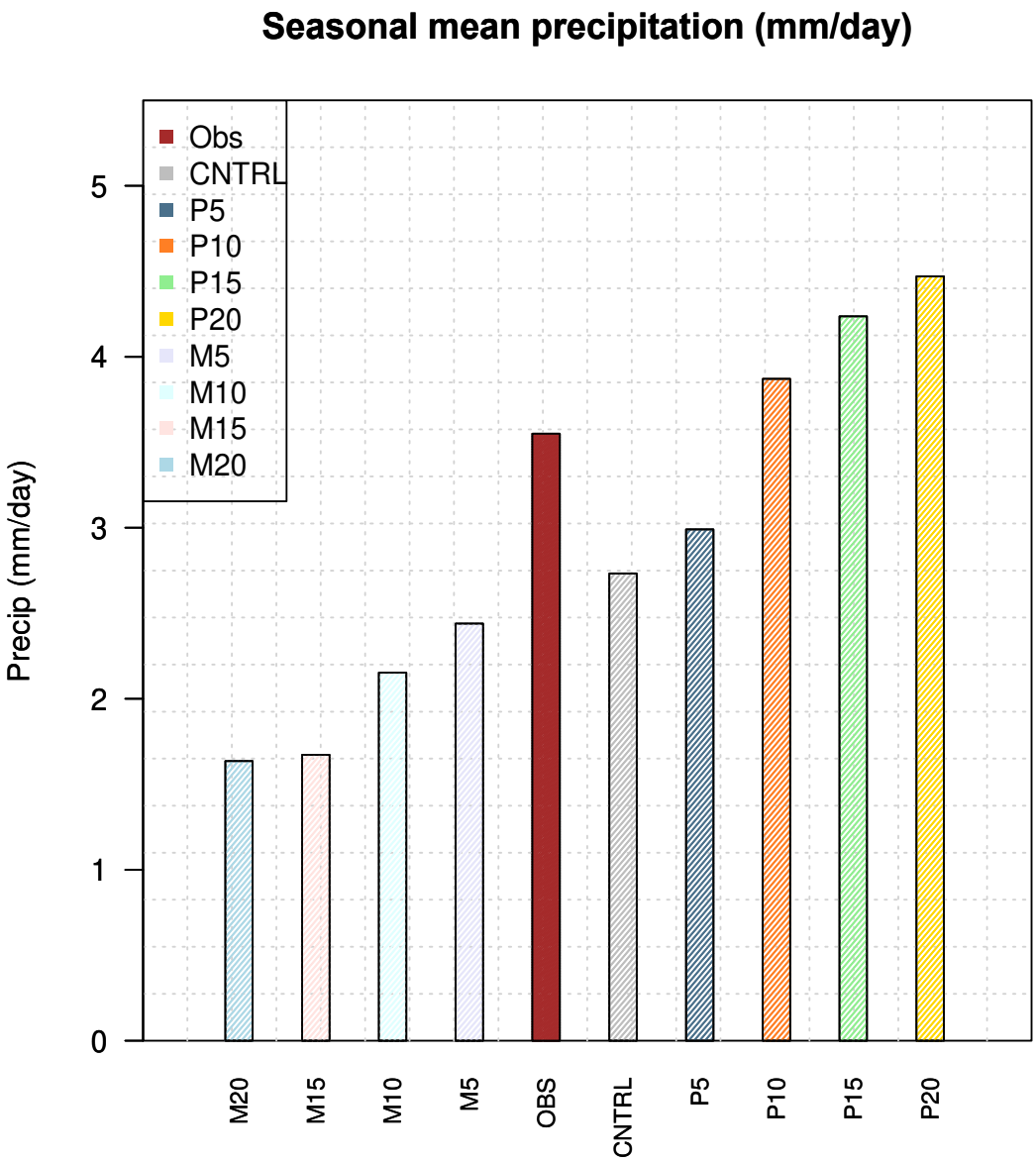

Figure 8: Seasonal (DJF) precipitation (mm/day) obtained from a) IMD gridded data, and RegCM simulations with different Himalayan orography representations (CNTRL, P5, P10, P15, P20, M5, M10, M15 and M20) for total nine distinct winter seasons (three years each for wet, normal and dry).

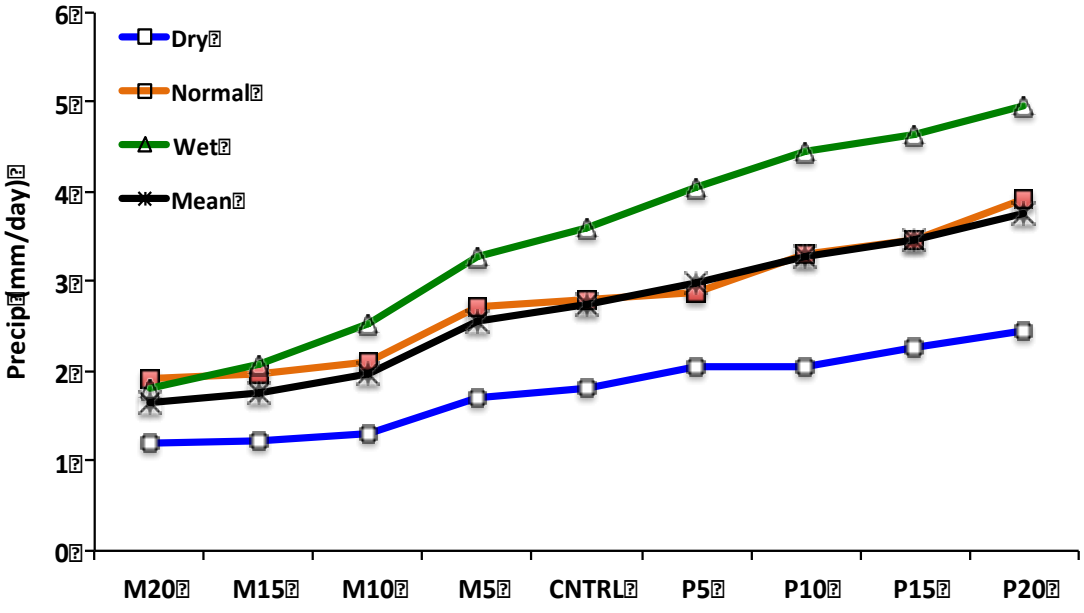

Figure 9: RegCM4 simulated area averaged (72°E-81°E; 29°N-37°N) seasonal (DJF) mean precipitation computed for different mean height of the Himalayan mountain representations (CNTRL, P5, P10, P15, P20, M5, M10, M15 and M20) respectively.

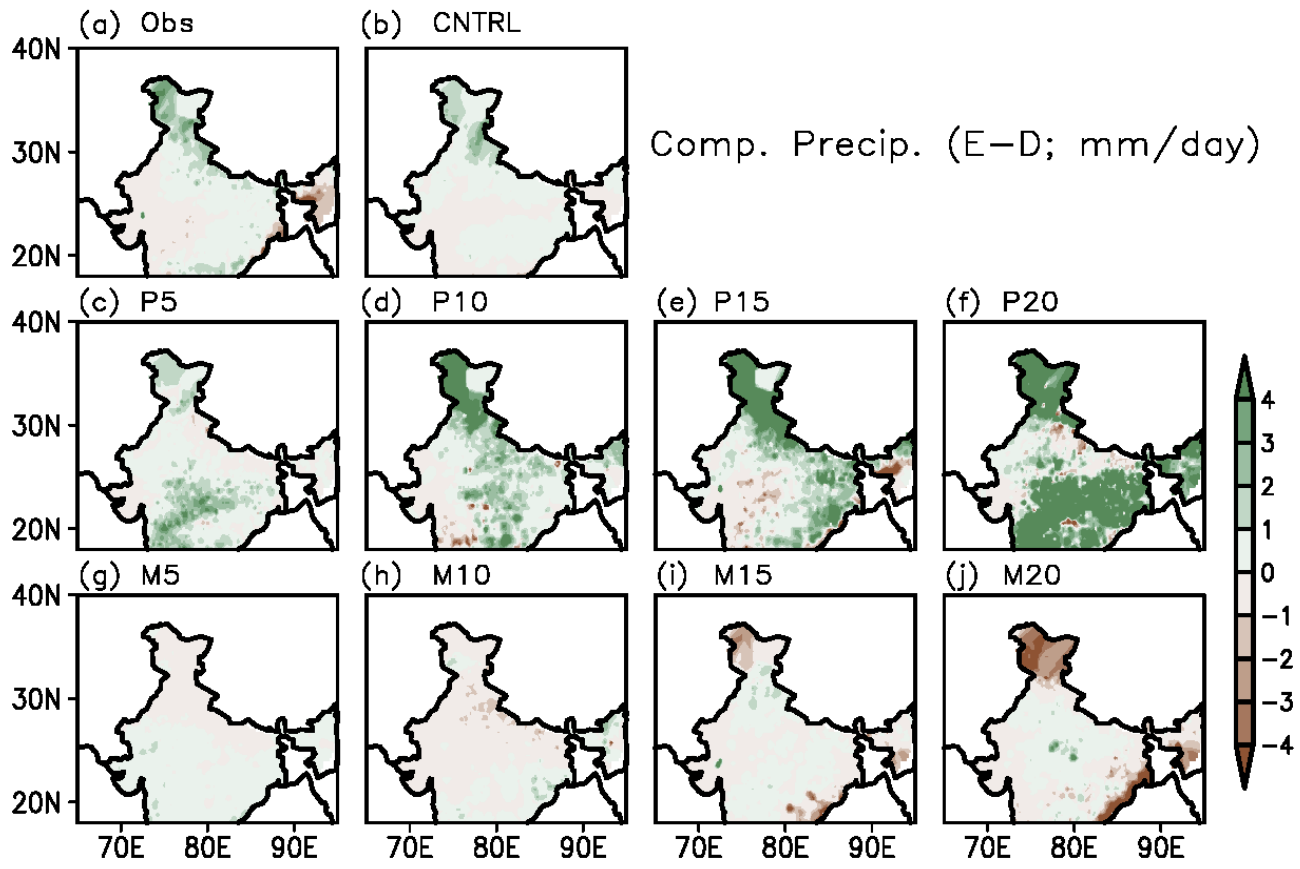

Figure 10: Seasonal mean (DJF) differences between wet- and dry-year composites of precipitation (mm/day) of (a) IMD observation, model simulations using (b) CNTRL, (c) P5, (d) P10, (e) P15, (f) P20, (g) M5, (h) M10, (i) M15 and (j) M20 heights respectively.

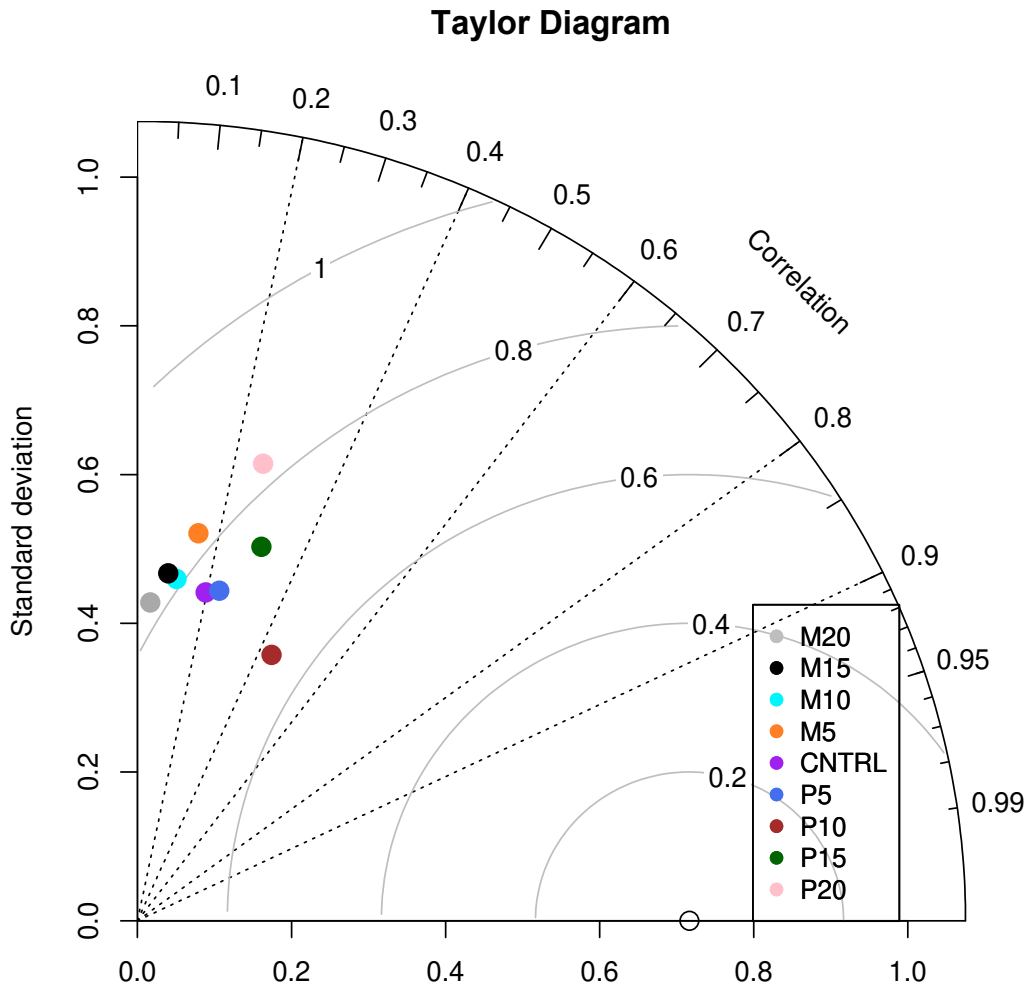

Figure 11: Taylor diagram for the north India average precipitation prediction skill of the different Himalayan orography representations.

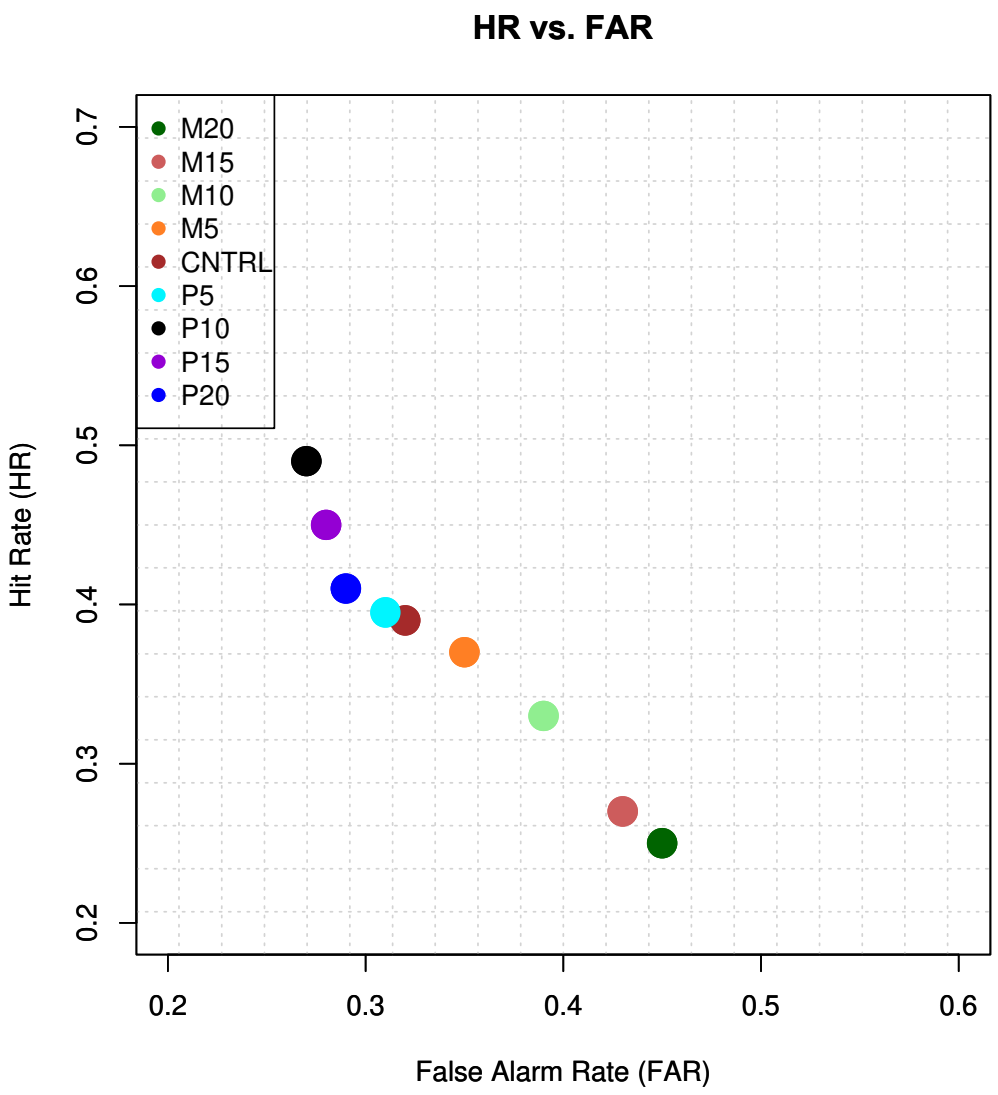

Figure 12: Hit rate versus False alarm rate statistics computed for NWI region for nine different sets of Himalayan orography representations.

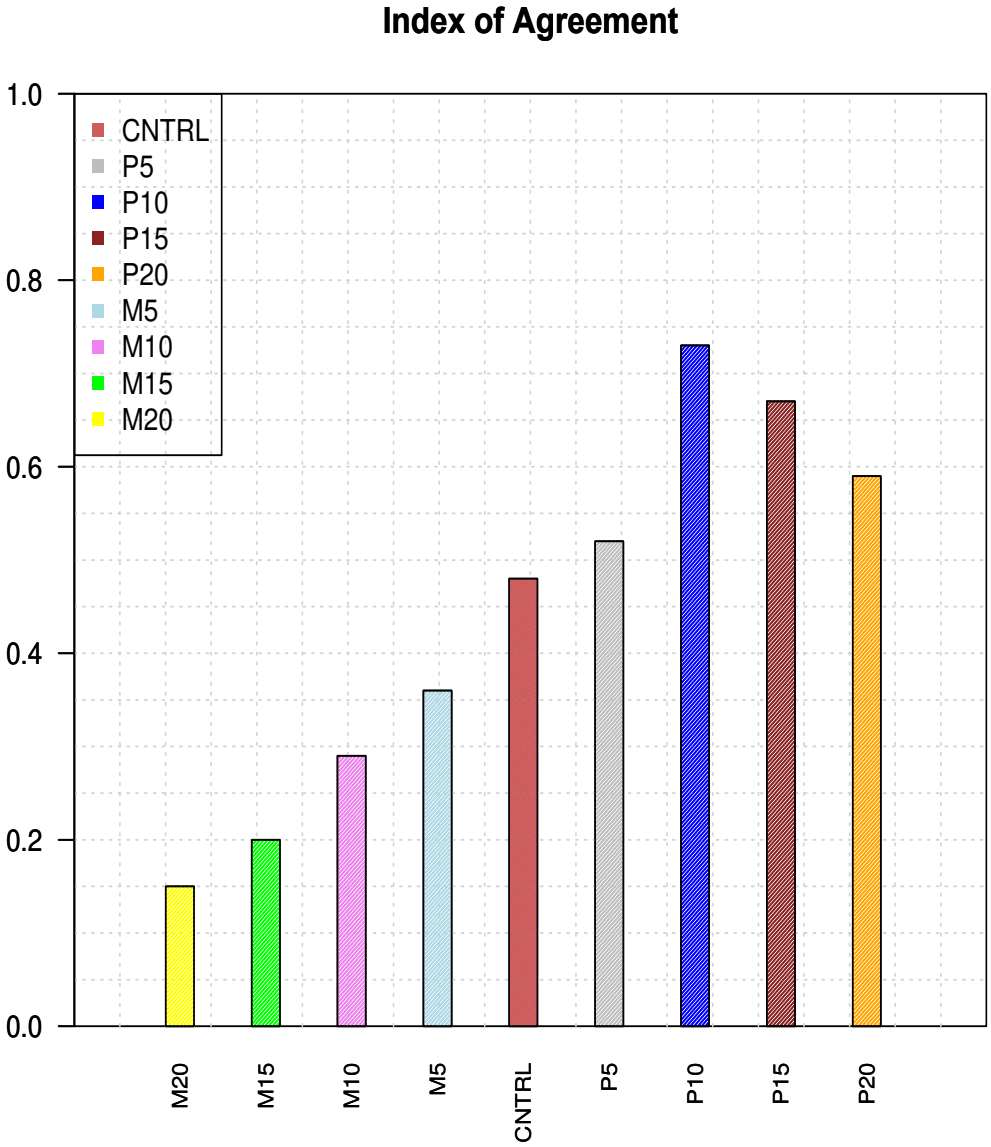

Figure 13: Willmott's index of agreement computed for NWI region for nine different sets of Himalayan orography representations.

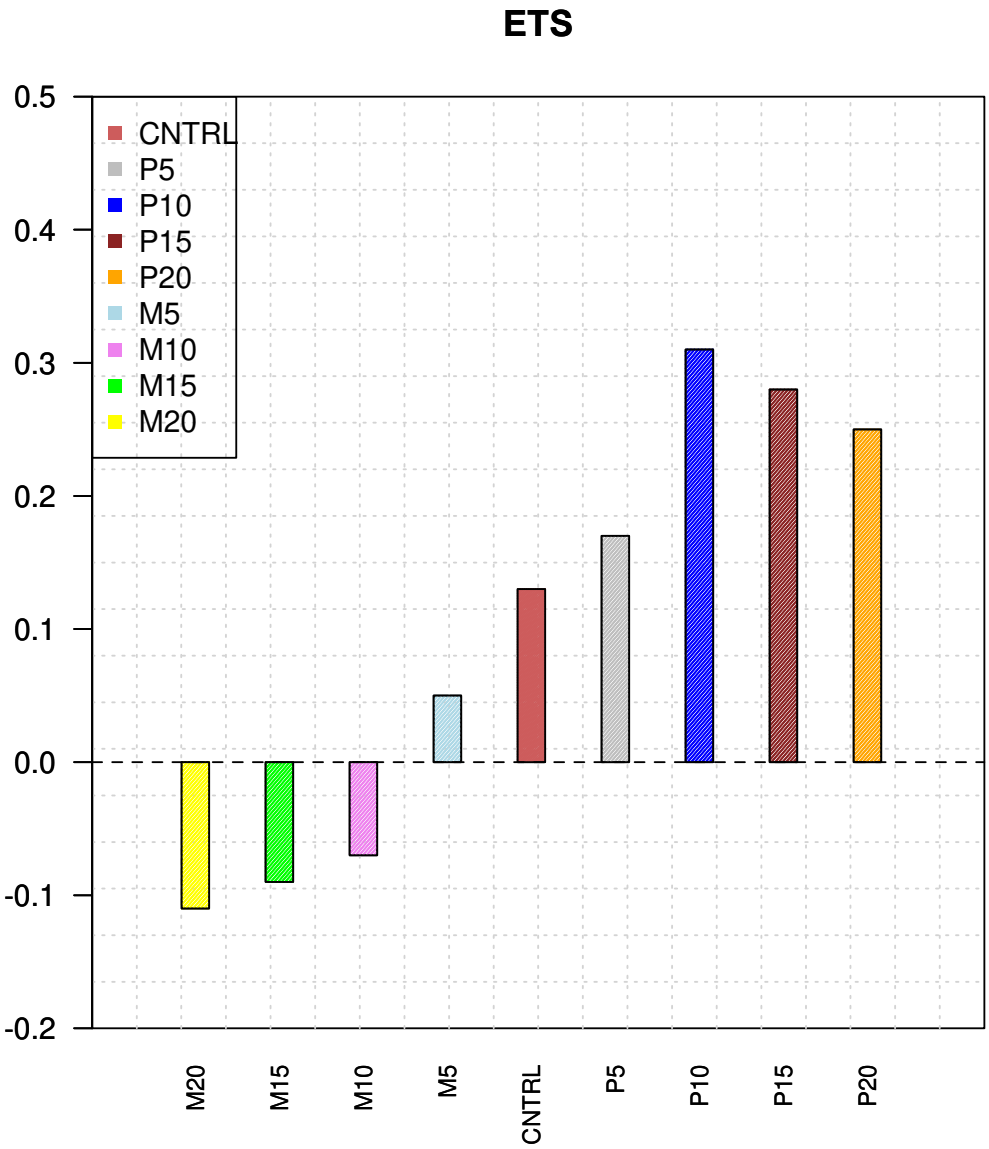

Figure 14: Equitable threat score (ETS) computed for NWI region for nine different sets of Himalayan orography representations.

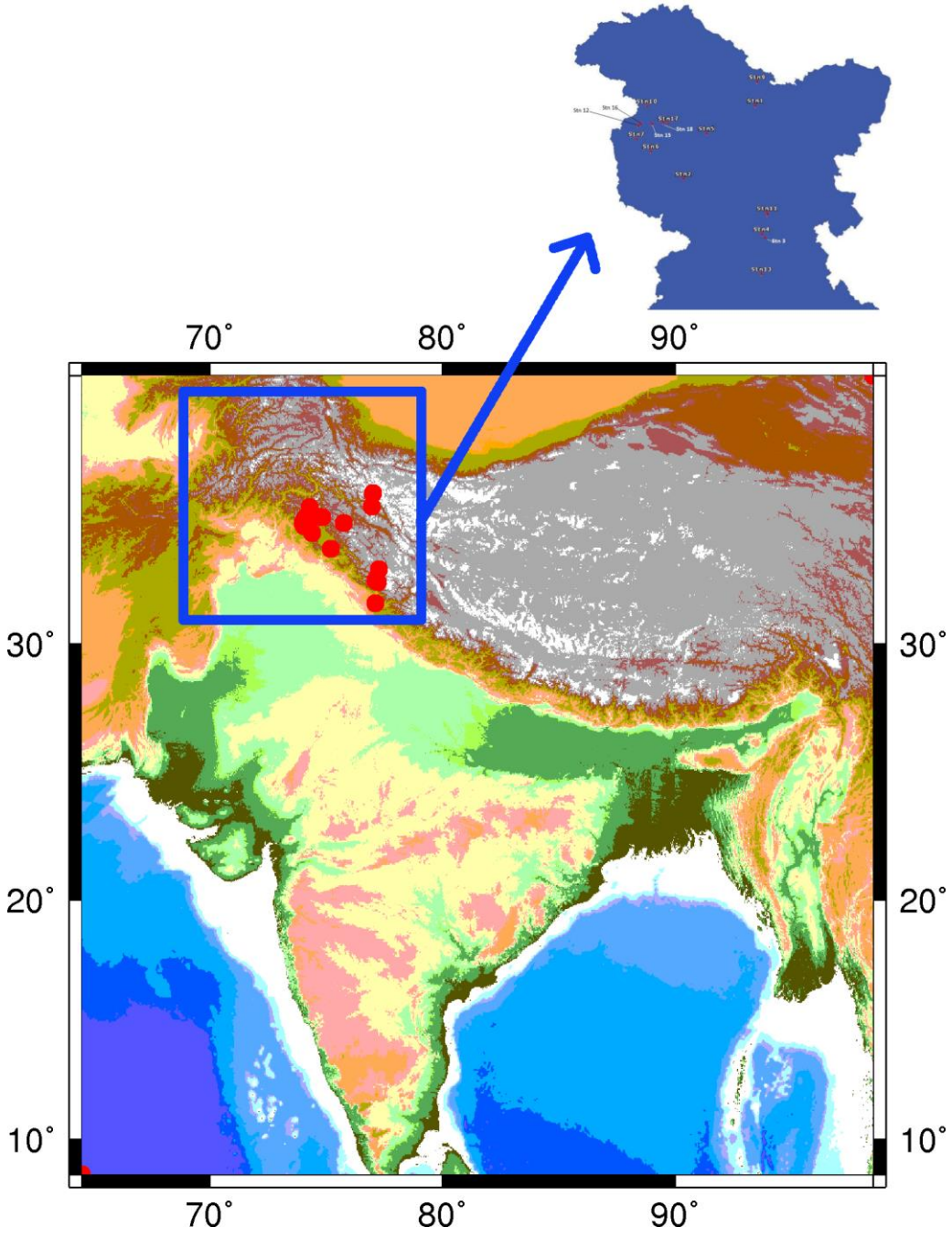

Figure 15: Geographical location of 17 SASE stations situated in the IWH region. (Source: The color geographical generated from http://woodshole.er.usgs.gov/mapit).

Table 1: Configuration of RegCM4 model used in the present study.

Dynamics	Hydrostatics
Main Prognostic Variables	u, v, t, q and p
Number of horizontal grid points	320 grid points along latitude and 416 grid points along longitude
Central point of domain	Latitude: 15.1^0N, longitude: 74.5^0E
Horizontal grid distance	30 km
Map projection	Lambert Conformal Mapping
Vertical co-ordinate	Terrain-following sigma co-ordinate
Cumulus parameterization	Grell with Fritch & Chappell closure (Grell 1993; Fritch and Chappell 1980)
Land surface scheme	Community Land Model (CLM3.5) (Oleson *et al.* 2008; Tawfik and Steiner 2011)
Orography treatment	Envelop orography (±5%, ±10%, ±15% and ±20% respectively from model mean height)
Radiation parameterization	NCAR/CCM3 radiation scheme (Kiehl *et al.* 1996)
PBL parameterization	Holtslag *et al.* (1990)

Table 2: Seasonal precipitation over seventeen stations obtained from SASE observation and RegCM4 model simulation with CNTRL and P10 experiments for composite of wet and dry years. The precipitation among the RegCM4 experiments close to SASE observation is represented in shade.

Station	**Composite wet**			**Composite dry**		
	SASE	***CNTRL***	***P10***	***SASE***	***CNTRL***	***P10***
1. Bahadur	**3.72**	2.31	4.56	**2.14**	1.45	2.36
2. Banihal	**7.62**	4.69	7.71	**3.05**	1.57	3.14
3. Bhang	**4.79**	4.71	8.43	**1.28**	2.34	5.48
4. Dhundi	**7.21**	3.09	7.26	**4.69**	3.28	4.75
5. Dras	**6.88**	4.96	6.95	**1.76**	1.69	4.39
6. Gulmarg	**7.23**	3.64	7.34	**4.09**	3.75	4.13
7. H-Taj	**7.89**	7.91	8.73	**2.31**	1.24	2.39
8.Kanzalwan	**9.83**	5.03	9.89	**3.79**	2.11	5.53
9. Kumar	**2.31**	2.37	6.14	**0.83**	1.01	3.91
10. Neeru	**5.07**	3.42	7.47	**2.72**	1.31	8.26
11. Patsio	**3.43**	2.59	6.01	**1.88**	2.76	5.43
12. Pharki	**8.96**	6.43	8.94	**4.69**	4.58	4.56
13. Solang	**8.67**	6.51	8.75	**3.35**	1.35	4.39
14. Stg-II	**10.51**	10.48	10.54	**3.71**	2.12	5.47
15. Z-Gali	**7.06**	3.54	8.85	**4.18**	3.69	4.23
16. Gugaldhar	**6.92**	3.69	7.05	**3.63**	2.86	7.89
17. Dawar	**4.58**	2.23	6.52	**2.85**	2.73	6.51